# Efficient Dynamic Routing and Spectrum Assignment for Multifiber Elastic Optical Networks

Jingxin Wu, Suresh Subramaniam, and Hiroshi Hasegawa

***Abstract*—Elastic optical networks are seen as a promising solution to improve spectrum utilization efficiency by utilizing flex-grid optical orthogonal frequency division multiplexing technology and facilitating flexible bandwidth allocation to services with heterogeneous demands. With dramatic growth of Internet traffic and imminent fiber capacity exhaustion, multiple fibers per link are required to accommodate increasing demands. In this paper, we investigate path selection and spectrum management for heterogeneous bandwidth requests by taking the network topology and expected traffic pattern into account. A novel and efficient solution for path selection and spectrum assignment that optimizes the state of the network after assignment is proposed. We first develop integer linear programming formulations to calculate path selection probabilities offline. Then, we propose a spectrum partition scheme that provides a particular spectrum range for each request size. A next-state-aware spectrum assignment algorithm with resource sharing among partitions is then introduced. We use the demand blocking ratio for dynamically arriving requests as the performance indicator. Simulation results indicate the effectiveness of our proposed schemes for routing and spectrum assignment, as they perform 1 to 2 orders of magnitude better than several baseline schemes.**

***Index Terms*—Fragmentation; Heterogeneous bandwidth; Multifiber elastic optical network; Network planning; Routing and spectrum allocation; Spectrum management.**

## I. Introduction

Optical orthogonal frequency division multiplexing (OOFDM)-based elastic optical networks are suitable for enhancing spectrum utilization efficiency [1]. In OOFDM, the fiber bandwidth is carved up into bands whose center frequencies (subcarriers) are spaced only a few GHz apart, with subcarrier bit rates of a few Gbps. This is to be contrasted with the conventional fixed-grid wavelength division multiplexing (WDM) technology, where the wavelength spacing is fixed, e.g., 50 GHz, and the wavelength bit rates are 10, 40, or 100 Gbps. By introducing the fine-grained grid, OOFDM allows allocated fiber bandwidth to better match traffic demands. Therefore, networks employing OOFDM are called elastic optical networks (EONs).

The routing and wavelength assignment (RWA) problem in WDM networks evolves into the routing and spectrum assignment/allocation (RSA) problem in EONs. The objective of RSA is to find a number of unoccupied frequency slots (FSs) to meet traffic demands and establish lightpaths [2–4]. The main constraints of the RSA problem are spectrum contiguity, spectrum continuity, and spectrum nonoverlapping. The spectrum contiguity constraint ensures that the FSs allocated to a lightpath are contiguous. The spectrum continuity constraint ensures that the same FSs are allocated on every fiber along the route. The spectrum nonoverlapping constraint ensures that any FS on any fiber is allocated to at most one lightpath. The RSA problem can be divided into two subproblems: the routing problem and spectrum allocation (SA). For the static/offline RSA problem, the normal objective is to minimize the maximum slot index (MS) while provisioning all traffic requests. For the dynamic RSA problem, the typical objective is to minimize the blocking ratio or demand blocking ratio (i.e., ratio of blocked bandwidth to total bandwidth requirement) of traffic requests.

The first comprehensive study on the RSA problem is [2], which formally defined the problem and proved its NP hardness. In order to solve the RSA problem efficiently, many heuristics have been proposed in the literature. Dealing with routing and spectrum allocation problems jointly usually requires high complexity [5–7]. Many papers in the literature solve this problem by decomposing it and solving the two subproblems in sequence. The shortest path with maximum spectrum reuse algorithm and a balanced load spectrum allocation algorithm (which determines the routing by balancing the load in the network) is proposed in [2] to solve the static RSA problem. In [8], given a set of traffic requests, the authors try to find disjoint paths to route requests in order to increase slot reuse in SA. For the dynamic RSA problem, bandwidth fragmentation and spectrum misalignment caused by dynamic setup and tear-down of traffic requests hurt the network performance. Many RSA schemes have been proposed to mitigate the bandwidth fragmentation issue [9–15]. Defragmentation algorithms that reroute connections are developed in [16,17]. Another scheme to eliminate

Manuscript received November 5, 2018; revised February 11, 2019; accepted February 11, 2019; published April 2, 2019 (Doc. ID 351117).

J. Wu (e-mail: jingxinwu@gwu.edu) and S. Subramaniam are with the Department of Electrical and Computer Engineering, George Washington University, Washington, DC 20052, USA.

H. Hasegawa is with the Department of Electrical Engineering and Computer Science, Nagoya University, Furo-cho, Chikusa-ku, Nagoya 464-8603, Japan.

https://doi.org/10.1364/JOCN.11.000190

 

bandwidth fragmentation without rerouting connections is to partition the spectrum for heterogeneous bandwidth demands. In [18,19], different partition schemes are investigated, and the well-known first-fit spectrum allocation is used. In [20], the spectrum is partitioned by classifying connection groups. All the above RSA schemes are proposed for EONs with a single fiber per link.

Internet traffic continues to grow dramatically due to emerging applications, such as livestreams and social networking. According to [21], global Internet traffic is expected to be more than 60 TBps in 2020. To accommodate increasing traffic demands, deploying multiple fibers on a physical link is needed. The wavelength/slot assignment in networks with multifiber links differs from prior schemes for single-fiber networks in that multifiber links provide more flexibility in switching wavelengths/frequency slots. The WA problem in multifiber WDM networks has been explored in the literature [22–28]. References [22,23] take the network state information into consideration and show good performance. Different cost functions based on the network state are utilized in the literature. Due to the heterogeneity of demands in EONs, which fiber to use on each link matters and will cause unnecessary fragmentation if not carefully addressed. In order to fully utilize the flexibility in multifiber links while satisfying constraints introduced by EONs, an efficient RSA scheme is necessary. Reference [29] proposes a multifiber-based RSA method by designing costs to first select routes and then spectrum slots and first-fit fibers to accommodate requests.

In this paper, we propose a novel and efficient solution for the dynamic RSA problem in multifiber elastic optical networks. Given a network and dynamic stochastic connection request arrivals with known/forecasted traffic loads, the problem is to assign a route and spectrum to each request, so that the blocking probability is minimized. Each link in the network contains multiple fibers. A network planning formulation based on the topology information is proposed so that the candidate paths for each source-destination node pair can be selected according to certain predetermined probabilities. Due to the heterogeneous request bandwidths, a partition scheme is applied so that each request size can use a particular spectrum range. In this case, each fiber can be viewed the same, and fiber selection on each link can also be avoided. Given the spectrum partitioning, an SA algorithm based on the network state information and the path selection probabilities is proposed. The next-state-aware SA algorithm is further improved by considering resource sharing among different partitions. For each arriving request, a routing path is first selected according to the precomputed probabilities; then, the next-state-aware SA is performed to assign contiguous FSs to that request. If there are no available FSs, the request will be blocked. We use the demand blocking ratio (ratio of the sum of bandwidths of blocked requests to total bandwidth of all requests) to indicate network performance.

An abstract of this paper was published in [30], which outlines the basic idea of our solution and presents one set of preliminary evaluation results. In this paper, we describe the details of our methods and present extensive evaluation results, including results from sensitivity tests. Our contributions are (1) we propose a multipath selection method for the routing problem, (2) we utilize a spectrum management scheme to alleviate fragmentation caused by heterogeneous request bandwidths, (3) we propose a spectrum assignment method that optimizes the state of the network *after* the assignment, and (4) we demonstrate through extensive simulations the effectiveness of our proposed schemes.

The rest of the paper is organized as follows. Section II gives the background and problem definition. Section III addresses the routing problem and introduces the multipath selection scheme. Section IV explains the spectrum management scheme, the next-state-aware SA algorithm for dedicated partitions, and an enhanced version with resource sharing among partitions. Performance evaluation results of the combined routing and spectrum allocation schemes are shown in Section V. Section VI concludes the paper.

## II. Background

Consider a network $\mathcal{G} = (\mathcal{V}, \mathcal{E})$, where $\mathcal{V}$ denotes a set of optical cross connects (OXCs), and $\mathcal{E}$ denotes a set of physical links. We assume that end nodes are connected to each OXC so that every OXC can be the origin or destination of connection requests. Each link contains multiple fibers, and the number of fibers on each link may be different. The spectrum resource on each fiber is carved up into frequency slots, with a bandwidth of 12.5 GHz each. All fibers consist of the same number of FSs. At each OXC, assume there are no switching constraints from input fibers to output fibers, i.e., any FS on an input fiber can be switched to the *same* FS on any of the output fiber.

A connection request to the network is an end-to-end lightpath with a source node, a destination node, and a data rate requirement. The number of FSs assigned to a request depends on the data rate requirement and the modulation format. In this work, we do not consider different modulation formats for different path lengths and assume the same modulation format is used as in [31]. Thus, the bandwidth demand for each connection only depends on the data rate requirement, and a connection request can be represented by a three-tuple (*source, destination*, $b$): a source node, a destination node, and a request size in terms of number of contiguous FSs. Heterogeneous traffic requests with different data rate requirements will consume a different number of FSs, which cause the fragmentation issue.

The routing and spectrum assignment (RSA) problem in multifiber EONs is to find a path and a set of contiguous FSs on *some* fiber on links along the path for an arriving request.

Spectrum management, such as partitioning the spectrum into dedicated ranges, is motivated by the heterogeneous request sizes. Let us take a look at a simple

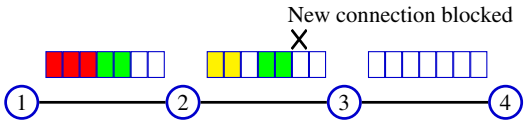


Fig. 1. Slot usages without spectrum management.


Fig. 2. Slot usages with spectrum management.

example with request sizes of two and three slots. If there is no spectrum management based on request classification, and first-fit spectrum/slot assignment algorithm is used for the requests; the network status is as shown in Fig. 1. When a new request of size 3 from node 2 to node 4 arrives, there are no available FSs, and this request will be blocked. On the other hand, with proper spectrum management, such as dedicating the first four slots for requests of size 2 and the last three slots for requests of size 3, for the same set of requests, the slot assignments will change and the new arriving request can be accommodated. Figure 2 shows the new assignments when utilizing spectrum management.

## III. Multipath Selection Scheme

A path between the source and destination nodes should be determined to accommodate the request. Commonly used routing schemes such as using a precomputed fixed single shortest path or one of many paths selected dynamically (based on the network state each time a request arrives) suffer from either poor performance (in the former case) or high computation complexity (in the latter case). We would like to fully utilize multiple paths between each node pair efficiently. Our proposal is to select a routing path based on some predetermined rules instead of calculating the best path each time for a new arrival request.

Given the traffic loads, we propose to compute a set of candidate paths and the path selection probabilities for each node pair *offline*. This approach fully utilizes the multiple paths between each node pair while keeping computational complexity quite low. Given the network topology and traffic loads for each node pair, the selection probabilities for all candidate paths are computed offline via a mixed-integer linear program to span loads over fibers. The result of this is that we obtain the probability distribution of the path to be selected for a request from $s$ to $d$, $p^k_{(s,d)}$, the probability that the $k$th path should be selected for node pair $(s,d)$. Each time a request arrives at the network, a path is selected to accommodate the request according to these predetermined probabilities.

### A. Notations

The input parameters are shown in Table I, including the detailed network topology information and the expected load for each route. The load for each route is based on the relative traffic intensities of the network and is assumed to be known from historical trends and/or traffic forecasts [32,33]. For example, if the source and destination of requests follow a uniform distribution, the load for each route can be set as 1.

TABLE I
Notation

| Symbol | Meaning |
|---|---|
| $N$ | Number of nodes in the network |
| $L$ | Number of links in the network |
| $e$ | Arbitrary network link |
| $F^e$ | Number of fibers on link $e$, $e \in \mathcal{E}$ |
| $R$ | Number of routes in the networks |
| $r$ | Arbitrary route |
| $W_r$ | Load for route $r$; depends on the traffic pattern; $W_r = 1, \forall r$ for uniform traffic |
| $K_r$ | Number of candidate paths for route $r$ |
| $k$ | Arbitrary candidate path |
| $A^e_{r,k}$ | = 1 if link $e$ is on the $k$th candidate path of route $r$; = 0, otherwise |

### B. Mixed Integer Linear Programming for Path Selection

We have derived mixed-integer linear programming formulations to compute the optimal probabilities of candidate paths for each route (source–destination node pair). Our objective is to minimize the sum of the average and maximum traffic load over all fibers (as opposed to links because different links may have different numbers of fibers) to balance the loads, so that the loads are distributed to fibers on different paths.

Objective: Minimize

$$\frac{1}{L}\sum_{e=1}^{L}\frac{\sum_{r=1}^{R} W_r y_r^e}{F^e} + \max_e \frac{\sum_{r=1}^{R} W_r y_r^e}{F^e}.$$

Variables:

(a) The probability of selecting the $k$th candidate path of route $r$:

$$0 \le p_r^k \le 1.$$

(b) The fraction of load for route $r$ that traverses link $e$:

$$0 \le y_r^e \le 1.$$

Constraints:

(a) The sum of candidate path selection probability for a given route should be 1.0. For all $r$,

$$\sum_{k=1}^{K_r} p_r^k = 1.$$

(b) The fraction of load for a route $r$ on a link is determined by the candidate path selection probabilities. For all $r, e$,

$$y_r^e = \sum_{k=1}^{K_r} A_{r,k}^e p_r^k.$$

## IV. Spectrum Assignment

When a request arrives, a path is selected to accommodate the request by simply using the probability distribution computed above. After a path is chosen for the arriving request, SA is performed to assign contiguous FSs to that request. If there are no available slots on the selected path, the request will be blocked.

### A. Spectrum Management

To mitigate the fragmentation caused by the mismatch of heterogeneous request bandwidths during the dynamic setup and tear-down of traffic, a dedicated partition for each demand size is utilized. The spectrum is partitioned into different segments, each dedicated to traffic requests with the same bandwidth.

We use the number of contiguous slots to represent the size of a request. Suppose there are $M$ different request sizes $b_j$, $j = 1, \ldots, M$. Then, the whole spectrum is partitioned into $M$ segments. The number of contiguous FSs dedicated to each segment is denoted by $P_j$, $j = 1, \ldots, M$. Let $S$ be the size of the whole spectrum, that is, the total number of FSs in a fiber. Then, the sizes of segments should meet the constraint: $\sum_{j=1}^{M} P_j = S$. In the segment for request set $j$, we have $P_j/b_j$ bins (a bin is a set of consecutive FSs of a fixed size that can accommodate one request of that size) in each fiber.

We assume that the connection size distribution is known (from traffic forecasts and historical trends), and let $\rho_j$ be the probability that an arbitrary arriving request is of size $b_j$: $\sum_{j=1}^{M} \rho_j = 1$. We present results later in this paper when the traffic forecasting is not completely accurate. This distribution is used to calculate the sizes of different segments as follows:

$$P_j = S \cdot \frac{\rho_j \cdot b_j}{\sum_{j=1}^{M} \rho_j \cdot b_j}. \tag{1}$$

The rationale behind this partition is to achieve spectrum fairness for different demand sizes. For example, suppose there are 352 FSs on each fiber, and there are three sets of requests with sizes $(b_1, b_2, b_3) = (3, 4, 7)$ and densities $(\rho_1, \rho_2, \rho_3) = (0.2, 0.5, 0.3)$. Then, according to Eq. (1), we get the segment sizes $(P_1, P_2, P_3) = (45, 152, 154)$, which correspond to 15, 38, and 22 bins for requests of sizes 3, 4, and 7, respectively, and 75 bins in total. The distribution of the number of bins for each request size is almost the same as the traffic distribution.

### B. Next-State-Aware Spectrum Assignment

In this section, we propose a next-state-aware (NSA) spectrum assignment algorithm based on the next state (i.e., the network state *after* the request is set up) and the path selection probabilities for requests, given the spectrum partitioning.

Because the whole spectrum has been partitioned into dedicated segments, each providing consecutive slots for a particular request size, the spectrum assignment problem can be addressed by assigning a bin in the segment specific to a request. In the $j$th dedicated segment of the spectrum, we have $P_j/b_j$ FS bins in each fiber. Suppose the request has a bandwidth requirement of $b_j$ FSs; the SA problem is to assign a bin of size $b_j$ for the request. The spectrum assignment problem is then transformed to select an available bin in the dedicated segment to accommodate a request without disrupting existing connections, so that the blocking probability is minimized.

For each new request, we only need to consider the network state corresponding to the specific spectrum segment, which this request size belongs to, based on the partitioning in the previous section. The network state denotes the current status of the network, i.e., the busy/free status of each slot in each fiber. Because dedicated partitioning has been determined, we only need to look at the status of each bin in that segment. In order to reduce the blocking probability, we should select a bin that can provide a "good" network state after the request is established.

In the rest of this section, we assume $X$ to be the number of bins in the segment the request belongs to. We first define the link capacity $c_e^x$ of link $e$ on bin $x$ in a network state as the number of fibers on which $x$ is unused on the link. Initially, in an empty network, $c_e^x = F^e, \forall x$. The path capacity is determined based on capacities of links along the path. For a path $k$, the path capacity on bin $x$ is defined as the least link capacity on bin $x$ along the path (which is also the link capacity of the most congested link along the path):

$$C_k^x = \min_{e \in \Xi(k)} c_e^x, \tag{2}$$

where $\Xi(k)$ is the set of links on path $k$. Then, the path capacity $C_k$ is the total capacity over all bins:

$$C_k = \sum_{x=1}^{X} C_k^x. \tag{3}$$

Because for each route (source–destination node pair) $r$ in the network, we have already determined the selection probabilities $p_r^k$ for each path candidate $k$, the capacity for that route is then defined as

$$C_r = \sum_{k=1}^{K_r} p_r^k C_k. \tag{4}$$

Then, the network capacity is defined as the total capacity over all routes $\sum_{r=1}^{R} C_r$.

Suppose a request is assigned to a candidate path $\kappa$. After the request is established on a bin in the spectrum segment, there may be capacity loss for other routes in the network. In order to leave the network in a desirable

state for future requests, we choose a bin that causes the least capacity loss among all available bins, to accommodate the current request. In order to calculate the capacity loss, we utilize the definition of conflict graph $\mathcal{G}' = (\mathcal{V}', \mathcal{E}')$, where each vertex $k \in \mathcal{V}'$ represents a path $k$ in the network, and an undirected edge $(k_1, k_2) \in \mathcal{E}'$ denotes that paths $k_1$ and $k_2$ share at least one link. Capacity loss can occur only for paths that contain common links with $\kappa$. So, when calculating the total capacity loss, we only need to look at paths that are connected to $\kappa$ in the conflict graph $\mathcal{G}'$. We use $\psi^\kappa$ to denote this set of paths.

Let us consider the total capacity loss $\zeta_x$ when bin $x$ is chosen for path $\kappa$. If at least one of the common links between $\kappa$ and a path $k' \in \psi^\kappa$ have the minimum capacity on bin $x$ along path $k'$, $C^x_{k'}$ will be decreased by 1 after the establishment of the request. Otherwise, when all common links between $\kappa$ and $k'$ have capacity larger than the current path capacity $C^x_{k'}$, the link capacity decrement of the common links caused by the request establishment will not affect $C^x_{k'}$, and there will be no capacity loss for path $k'$. We use $\upsilon_{k'}$ to denote the capacity loss for path $k'$. Taking the path selection probability into account, if path $k'$ belongs to route $r$ and the probability of selecting $k'$ for $r$ is $p^{k'}_r$, then $\upsilon_{k'}$ is equal to either $p^{k'}_r$ or 0, depending on the network state. The total capacity loss after bin $x$ is chosen will be $\zeta_x = \sum_{k' \in \psi^\kappa} \upsilon_{k'}$. We assign to the request the bin $x^*$, which causes the least capacity loss, i.e.,

$$x^* = \arg \min_{x \in \Omega(\kappa)} \zeta_x, \tag{5}$$

where $\Omega(\kappa)$ is the set of available bins in path $\kappa$ for the request.

We illustrate our proposed SA method with the help of a small five-node network, as shown in Fig. 3. There are five nodes and six links in the network. The number of fibers is 5, 5, 3, 4, 3, 2 on bidirectional links (1, 2), (1, 3), (2, 4), (2, 5), (3, 4), (3, 5), respectively. Given the path candidates for each route and a uniform traffic pattern, based on the multipath selection formulation, we obtain the probabilities as in Table II.

When a new request from source node 2 to destination node 5 arrives, from Table II, path 2–5 is selected. Then, we check the network state of the spectrum segment this request belongs to. Based on the conflict graph, we can see that only paths 1–2–5, 4–2–5, and 2–5–3 have common links with path 2–5. Suppose there are four bins $x_1, x_2, x_3, x_4$ in the segment, and that the current network states are as shown in Fig. 4. The number attached to each link denotes the current link capacity on a bin, which is the number of fibers on which the bin is free.

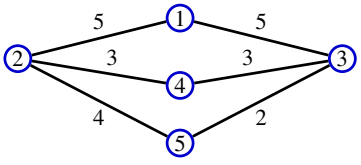


Fig. 3. Small five-node network to illustrate our proposed SA method.

TABLE II
PATH SELECTION PROBABILITIES FOR THE SMALL NETWORK

| Route | Candidate Paths | Selection Probability |
|---|---|---|
| 1–2 | 1–2 | 1.0 |
| 1–3 | 1–3 | 1.0 |
| 1–4 | 1–2–4 | 1/3 |
| | 1–3–4 | 2/3 |
| 1–5 | 1–2–5 | 1.0 |
| | 1–3–5 | 0.0 |
| 2–3 | 2–1–3 | 1.0 |
| | 2–4–3 | 0.0 |
| | 2–5–3 | 0.0 |
| 2–4 | 2–4 | 1.0 |
| 2–5 | 2–5 | 1.0 |
| 3–4 | 3–4 | 1.0 |
| 3–5 | 3–5 | 1.0 |
| 4–5 | 4–2–5 | 2/3 |
| | 4–3–5 | 1/3 |

Let us take bin $x_2$ as an example to see how the total capacity loss is calculated. Because link (2, 5) has the least link capacity along both paths 1–2–5 and 4–2–5, if $x_2$ is allocated to the new request, both path capacities will be decreased. According to the selection probabilities of these two paths, the capacity loss is 1.0 for path 1–2–5, and $\frac{2}{3}$ for path 4–2–5. For path 2–5–3, the selection probability is 0, so we do not need to take this path capacity into account. In total, the capacity loss is $\frac{5}{3}$ if bin $x_2$ is used. Similarly, capacity losses for $x_1, x_3, x_4$ are $1.0, 0, \frac{2}{3}$, respectively. Thus, bin $x_3$ will be allocated to accommodate this request.

### C. Resource Sharing Among Partitions

Dedicated spectrum partitioning is expected to mitigate the fragmentation issue; however, at low loads, dedicated partitions may lead to underutilization of the spectrum when there are no free bins in the segment corresponding to an arriving request, but there are free bins in other segments. In order to further improve spectrum efficiency, we consider resource sharing among partitions. For each

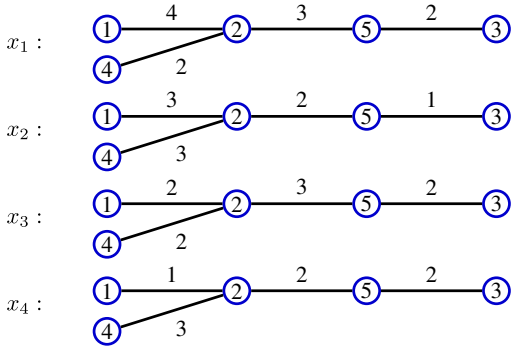


Fig. 4. Network state example: link capacities of a partial network on bin $x_1, x_2, x_3, x_4$.

request, we first check whether there is any available bin in the dedicated spectrum segment this request corresponds to. If no available bin exists in this segment, FSs in other partitions will be examined. In addition to the bin states in each segment, the occupancy states for each FS also need to be recorded, which are used to determine the candidate FS sets. We use the same assignment scheme as in the previous section, with slight modifications in the calculation of capacity loss. Take a candidate FS set $\chi$ as an example; it may be across multiple bins, and the first and/or last bins may only partially be in $\chi$. For the bins where all FSs are within $\chi$, the capacity loss calculation is the same as that in the previous section. For the first or last bin, if it has already been marked as occupied (which means some slots in the bin while outside $\chi$ are in use) because of preceding requests, the link capacity loss for this bin is set to 0. The total capacity loss will be the sum of the capacity loss for each bin in this candidate FS set. As before, the FS set that causes minimum capacity loss will be assigned to the request. If $\chi$ is the selection, all bins $\chi$ crosses will be marked as occupied.

The maximum number of hops in a path is $O(N)$, and the total number of FSs on each fiber is $S$. Thus, the time complexity of our algorithm is $O(S \cdot N^3)$ per request.

## V. Results

We present performance evaluation results for two real network topologies, the NSFNET (Fig. 5) and the Pan-European network (Fig. 6). The NSFNET consists of 14 nodes and 22 links, while the Pan-European network consists of 28 nodes and 43 links. Each link has a random number of fibers, uniformly distributed between five and 10 fibers. For the elastic optical network, we assume the fiber capacity of 352 frequency slots, with each slot having a bandwidth of 12.5 GHz.

The traffic demand is a set of dynamically arriving connection requests. Each request represents a connection between a pair of nodes in the network. Connection requests arrive at the network according to a Poisson process. Each request has a mean holding time of 1 (arbitrary time unit), and the arrival rate of traffic requests is varied in order to examine the network performance under varying offered loads. Frequency conversion is not considered in this paper. There are three types of demands with 40/100/400 Gbps, requesting three, four, and seven frequency slots, respectively [4]. The request size distribution is $(\rho_1, \rho_2, \rho_3) = (0.2, 0.5, 0.3)$. Based on this information, the spectrum partitioning can be determined. We use the demand blocking ratio of dynamic traffic requests to measure the performance in multifiber elastic optical networks. For each simulation, the results of 10 runs are recorded, with each run consisting of 1 million dynamic requests, excluding 10,000 warm-up requests. The average results with 95% confidence intervals are presented in the figures, which indicate that our results are relatively stable.

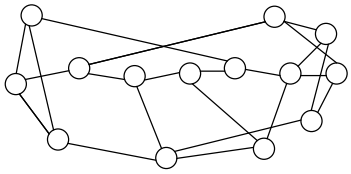

Fig. 5. 14-node NSF network.

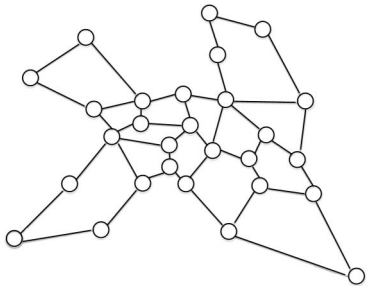

Fig. 6. 28-node Pan-European network.

Table III shows the notations of different routing and spectrum assignment schemes. SSP denotes the fixed single shortest-path routing scheme, while MPS denotes our proposed multipath selection-based routing scheme. DP represents the dedicated spectrum partition scheme, where each request size corresponds to one spectrum segment. SP is used to denote the improvement of a DP scheme with resource sharing among partitions. We use R to denote random slot set assignment, FF for first-fit SA, FLF for first last-fit SA, MK for one of the best schemes proposed in the literature [19], and NSA for our network-state-aware algorithm. R and FF provide slot assignment considering the whole spectrum without partitioning (NP) if not otherwise specified. In the FLF SA scheme [3], the whole spectrum is divided into several partitions, and requests attempt to use the lowest indexed FSs in the odd-numbered partitions and the highest indexed FSs in the even-numbered partitions to create opportunities for more contiguous FSs. In our simulations for FLF, we partition the whole spectrum into four segments, each of 88 FSs. The MK scheme proposed in [19] is designed for single-fiber links, and we adapt it to our multifiber link case. In MK, the same partitioning as in our proposed scheme and FF slot assignment in each partition is used. The resource sharing in MK is different, though each partition is shared by higher bandwidth requests only.

TABLE III
Notation of Schemes

| Notation | Scheme |
|---|---|
| SSP | Single shortest-path routing |
| MPS | Multipath selection routing scheme |
| NP | No partition scheme |
| DP | Dedicated spectrum partition scheme |
| PS | Dedicated partitions with resource sharing scheme |
| R | Random slot set assignment |
| FF | First-fit slot set assignment |
| FLF | First last-fit SA |
| MK | Spectrum partition and sharing scheme proposed in [19] |
| NSA | Next-state-aware SA |

We first evaluate our proposed schemes for dynamic connections with uniform traffic patterns. The source and destination nodes for each connection request are uniformly randomly selected. We present several results to highlight the improvement brought by each of the three novel strategies we propose, namely, multipath selection, spectrum partitioning with resource sharing, and next-state-aware slot assignment.

### *A. Evaluation of Multipath Selection Scheme*

Given the uniform traffic pattern, we obtain the path selection probabilities for each of the two networks. Figures 7 and 8 show the comparison between the performance (demand blocking ratio) of the baseline algorithm NP-FF-SSP and that of FF with our multipath selection scheme (MPS) for the NSFNET and Pan-European network, respectively. We can see that our routing scheme works much better than the fixed single shortest-path scheme. Because the selection probabilities can be precomputed via the ILP model offline and the runtime path selection can be implemented via a lookup table, the time complexity of choosing a path at runtime is negligible.

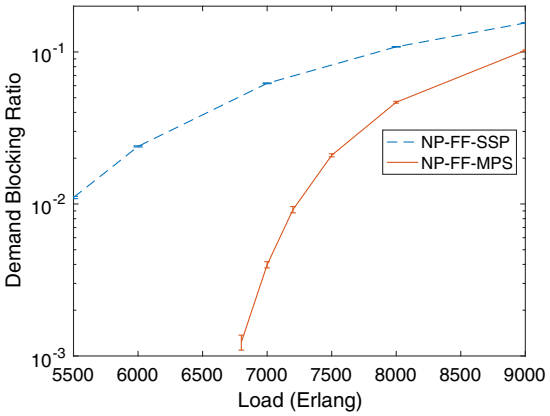


Fig. 7. Effectiveness of the multipath selection scheme in NSFNET.

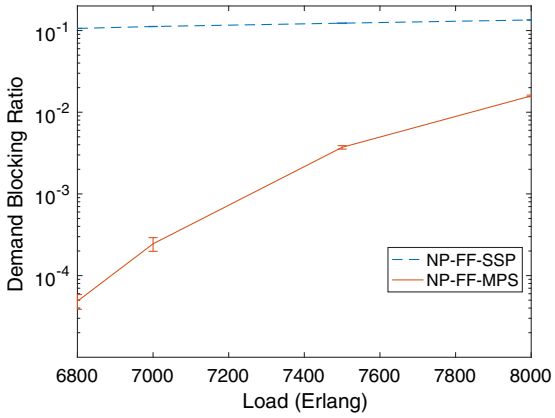


Fig. 8. Effectiveness of the multipath selection scheme in the Pan-European network.

TABLE IV
EXECUTION TIME OF MILP

| Topology | Number of Nodes | Number of Edges | K | Execution Time (s) |
|---|---|---|---|---|
| NSFNET | 14 | 22 | 4 | 0.02 |
| Pan-European | 28 | 43 | 4 | 0.03 |
| Random | 50 | 1000 | 4 | 8.33 |
| Random | 50 | 1225 | 4 | 12.15 |
| Random | 100 | 2000 | 4 | 50.83 |
| Fully connected | 100 | 4950 | 4 | 199.46 |

Nevertheless, to demonstrate the feasibility of solving the MILP offline for large topologies in a reasonable amount of time, we present in Table IV the execution times for solving the MILP for the two topologies considered in this paper as well as for randomly generated topologies, with a given number of nodes and edges, for uniform traffic. We can see that even fairly large instances can be solved within a few minutes. This is because the MILP is based only on the network topologies and traffic patterns and does not require the actual set of connection requests.

### *B. Evaluation of Spectrum Management and Assignment Scheme*

Figures 9 and 10 show the spectrum efficiency improvement caused by a dedicated spectrum partition. The baseline, NP-FF, is compared with the result of dedicated partition (DP) with FF spectrum assignment. Both use the single shortest-path routing (SSP). We can see that, even without resource sharing among partitions, there is steady improvement in spectrum efficiency. The spectrum underutilization for small workloads can be improved by resource sharing among different spectrum segments.

To evaluate the efficiency of our NSA algorithm, we first run simulations for traffic requests with a single size. The performance of NSA is compared with that of the baseline,

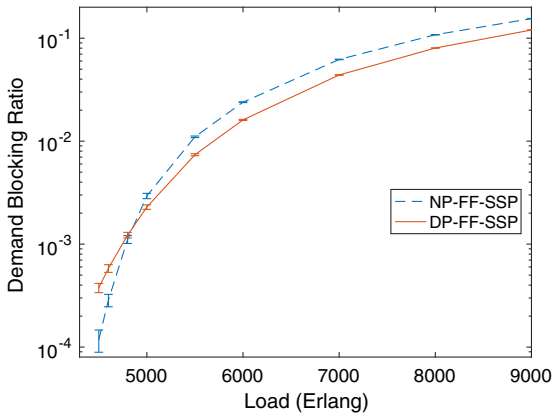


Fig. 9. Effectiveness of a spectrum partition in NSFNET.

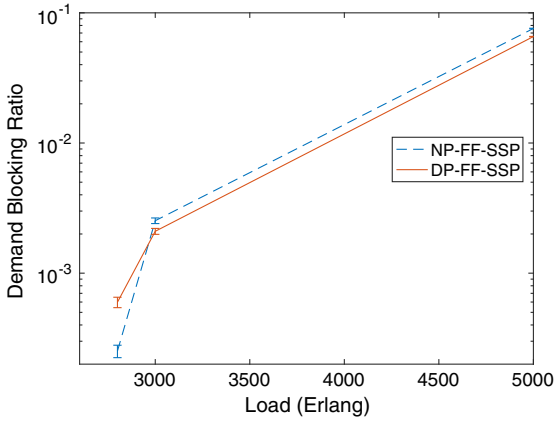


Fig. 10. Effectiveness of a spectrum partition in the Pan-European network.

FF. Both use the SSP. The first comparison is on a 10-node and 11-link sparse network (SPARSENET) with five to 10 fibers per link (topology not shown here). Figure 11 shows a huge spectrum efficiency improvement by utilizing NSA in SPARSENET. The second comparison is on the NSFNET. In Fig. 12, the spectrum efficiency improvement in the mesh network is not as large as in SPARSENET but still significant. This indicates that, when there are more overlapping paths (more common links), our algorithm works much better. From Fig. 12, we can see that there is still a 14%–32% performance improvement even when the topology is not sparse.

In networks with heterogeneous requests, the performance comparison of a joint dedicated spectrum partition and our proposed NSA algorithm with the baseline (NP-FF-SSP) is similar to Fig. 10. There is spectrum underutilization for small loads. Figures 13 and 14 show the spectral efficiency improvement by resource sharing among partitions. We can see a huge improvement in performance for low traffic loads.

Next, we present a comparison among several spectrum assignment schemes with SSP routing. Figures 15–17 show the results for the uniform traffic pattern in different networks. As expected, in schemes without dedicated

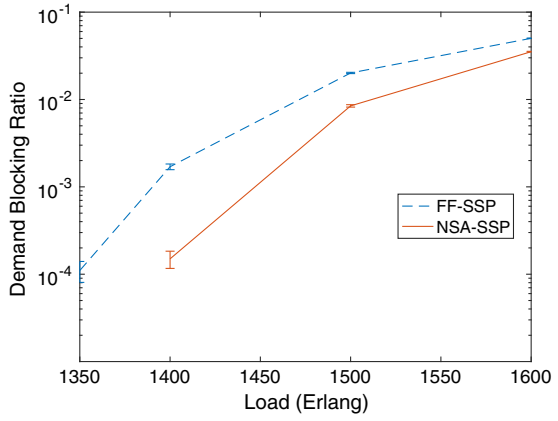


Fig. 11. Effectiveness of the NSA algorithm in SPARSENET.

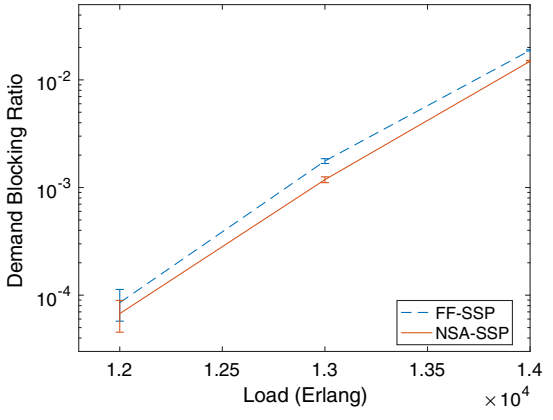


Fig. 12. Effectiveness of the NSA algorithm in NSFNET.

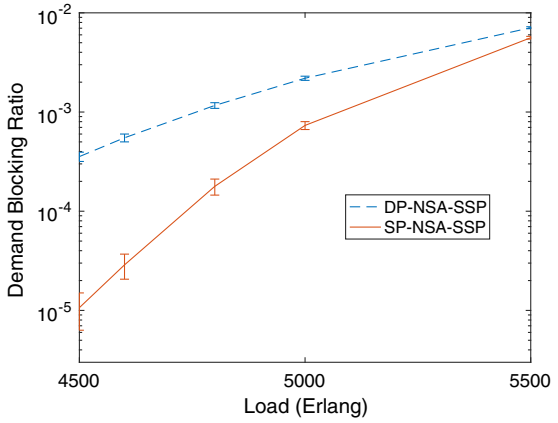


Fig. 13. Effectiveness of resource sharing among partitions in NSFNET.

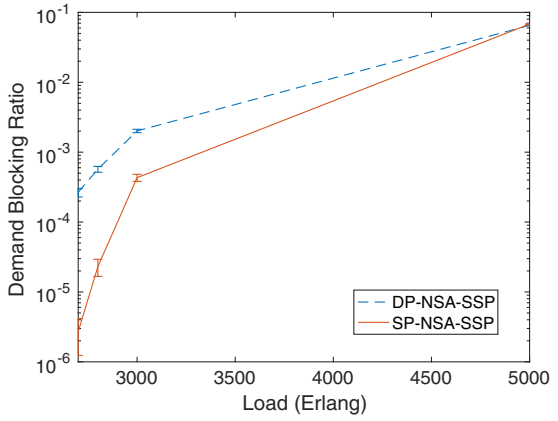


Fig. 14. Effectiveness of resource sharing among partitions in the Pan-European network.

partitioning, R always performs worst, and FLF performs better than FF by giving more contiguous aligned FSs. In low load cases, MK has higher demand blocking probability

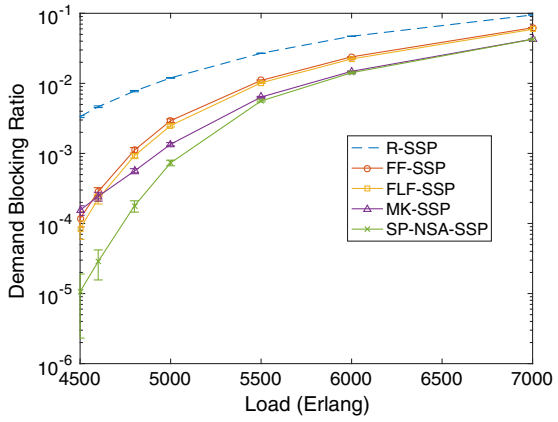


Fig. 15. Comparison of SA schemes in NSFNET.

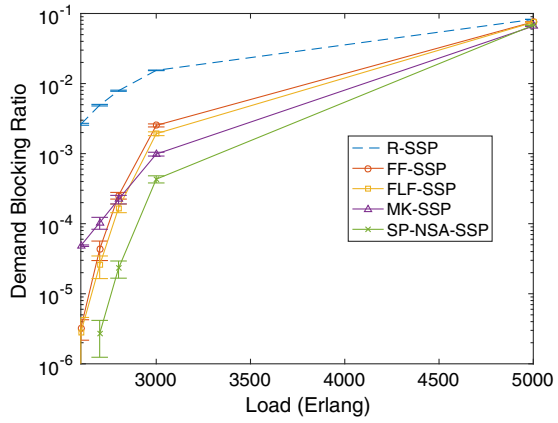


Fig. 16. Comparison of SA schemes in the Pan-European network.

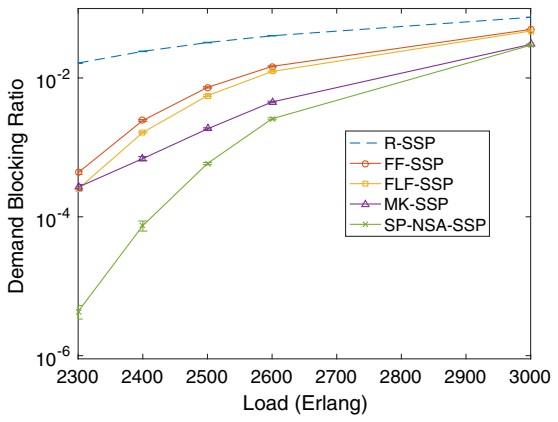


Fig. 17. Comparison of SA schemes in SPARSENET.

than FF and FLF due to its limited resource sharing and therefore resource underutilization. Then, the effect of spectrum management (decreased fragmentation) dominates in higher load cases, which leads to better performance of MK compared with FF and FLF. Our scheme takes all these aspects into account, performs spectrum allocation based on the global network states, and therefore exhibits superior performance.

### *C. Evaluation of the Joint Routing and Spectrum Assignment Scheme*

We conduct two sets of simulations to evaluate the joint effect of the multipath selection and the spectrum assignment schemes. According to the traffic pattern, a set of path selection probabilities is precomputed. We apply this multipath selection jointly with all spectrum assignment schemes in our evaluation.

We first show a set of simulation results for the uniform traffic pattern. Figures 18 and 19 show the performance comparison of our scheme with other baselines jointly with a multipath selection for the NSF and Pan-European networks. With the joint scheme, our algorithm still performs the best, and the same conclusions can be drawn. By comparing results in Figs. 15 and 18, we can see that, by jointly applying multipath selection with each spectrum assignment scheme, the demand blocking ratio greatly

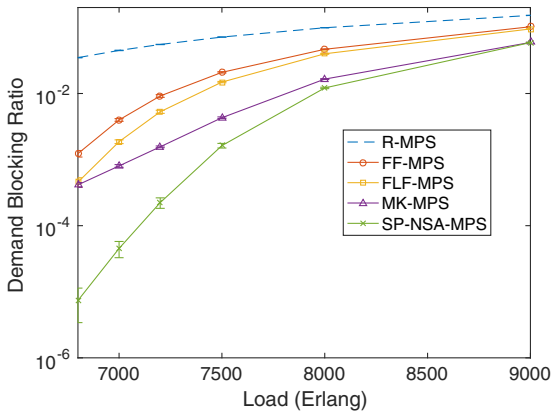


Fig. 18. Comparison of joint schemes in NSFNET with the uniform traffic pattern.

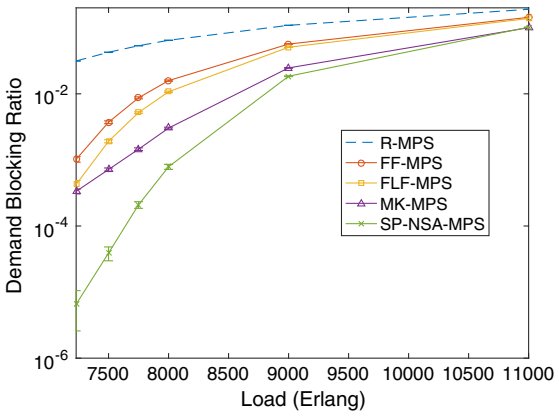


Fig. 19. Comparison of joint schemes in the Pan-European network with the uniform traffic pattern.

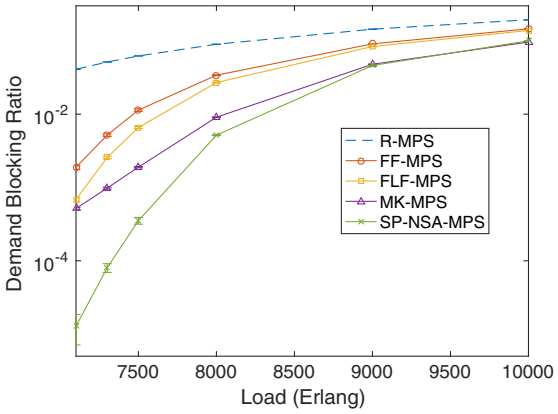


Fig. 20. Comparison of joint schemes in NSFNET with the nonuniform traffic pattern.

improves, and more load can be accommodated in the network.

The other set of simulations is conducted for a nonuniform traffic pattern, where the probability that each node is selected as source or destination $u_v, v \in \mathcal{V}$, can be different from each other. $\sum_{rv \in V} u_v = 1.0$. We assume nodes with higher connectivities have a larger volume of traffic, and the probabilities are proportional to the node degrees. The comparison results for both the NSF and Pan-European network are shown in Figs. 20 and 21, respectively. We can see similar trends as in the previous results. This further validates the effectiveness of our algorithm.

### *D. Sensitivity Evaluation*

We also conduct sensitivity tests to see how well our scheme performs when there is variation in the traffic pattern and demand size distribution. Figure 22 shows the test results corresponding to variation in demand size distribution in the NSF network with a uniform traffic pattern. The distribution of the three demand types is $(\rho_1, \rho_2, \rho_3) = (0.2, 0.5, 0.3)$ originally, and spectrum partitioning is calculated based

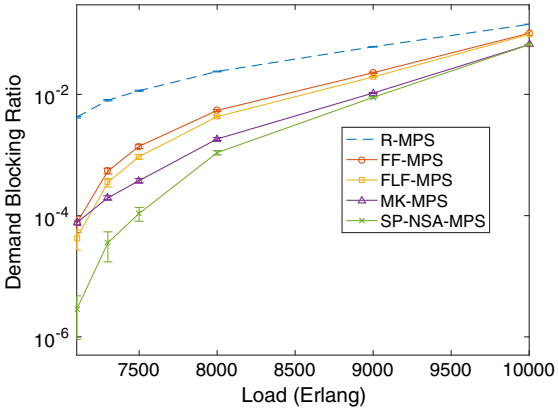


Fig. 21. Comparison of joint schemes in the Pan-European network with the nonuniform traffic pattern.

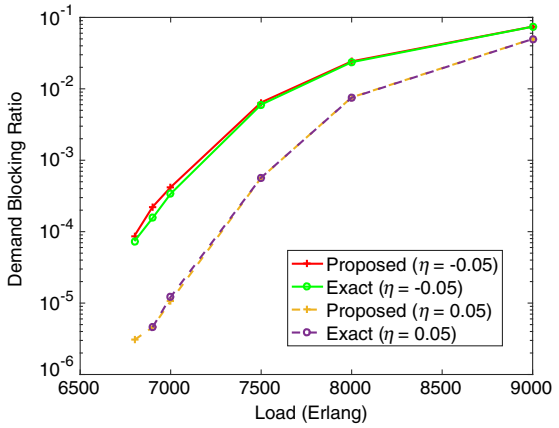


Fig. 22. Sensitivity test for the demand size distribution in the NSF network.

on this distribution. If there is a small change $\eta$ in the distribution $(\rho_1 + \eta, \rho_2 + \eta, \rho_3 - 2\eta)$, we compare the performance of applying the original spectrum partition to the changed traffic and that of applying the adjusted partition calculated based on exact distribution. The results are represented by "Exact" (with adjustment according to exact information) and "Proposed" (without exact information). The two sets ($\eta = -0.05$ and $\eta = 0.05$) show little performance degradation.

Figure 23 is the test result corresponding to perturbation in the traffic pattern in the NSF network. The demand size distribution does not change. The original probabilities that a node is selected as a source or destination are in proportion to the node degrees, and the multipath selection probabilities are calculated according to this nonuniform traffic pattern. If there is a small change $\eta$ in the probabilities $(u_1 + \eta, u_2 + \eta, \ldots, u_N - (N-1)\eta)$, we compare the performance of applying the original path selection to the changed traffic and that of applying the adjusted path selection calculated based on the exact traffic pattern. The two sets ($\eta = -0.01$ and $\eta = 0.01$) show little performance variation. We conclude that small variations in forecasted traffic do not affect the performance of our proposed algorithm significantly.

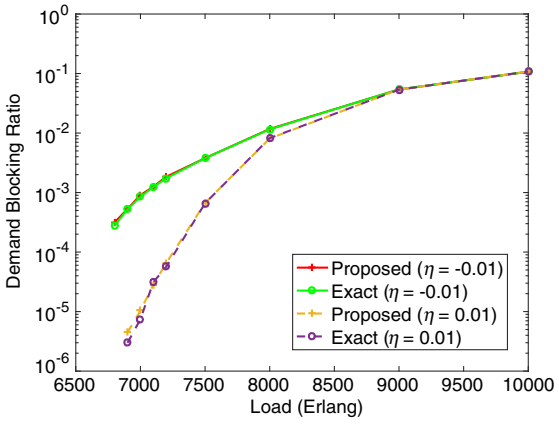


Fig. 23. Sensitivity test for the traffic pattern in the NSF network.

### *E. Extension to Multiple Modulation Levels*

In this section, we outline how our approach can be extended when multiple modulation formats are utilized and the selected modulation format is based on the length of the path. The only part of our scheme that requires modification is the calculation of the spectrum partition sizes. Due to the precalculated path selection probabilities, the known traffic pattern, link lengths, and the maximum distance reach for each modulation format, we can calculate the probabilities of required slots for each request size. Given these probabilities and the predicted connection size distribution, the spectrum partition sizes can be calculated.

Assume two modulation formats are utilized. The request size is in terms of number of contiguous FSs when using the higher modulation format. If the request selects a path exceeding a distance limit, it will consume more FSs in the lower modulation format.

Assume the probability that a request selects a path exceeding the distance limit is $\beta_m$:

$$\beta_m = \sum_{r=1}^{R} \phi^r \beta_m^r, \tag{6}$$

where $\phi^r$ is the probability for route $r$, and $\beta_m^r$ is the sum of the path selection probabilities of lengthy paths for route $r$. The sizes of different segments are updated as follows, with notations the same as in Section IV.A:

$$P_j = S \cdot \frac{(\rho_{j-1} \cdot \beta_m + \rho_j \cdot (1-\beta_m)) \cdot b_j}{\rho_M \cdot b_M + \sum_{j=1}^{M-1} \rho_j \cdot (1-\beta_m) \cdot b_j + \rho_j \cdot \beta_m \cdot b_{j+1}}. \tag{7}$$

For simplicity, we assume three types of demands: two requiring three and four FSs in DP-QPSK modulation format, and one requiring seven FSs in the BPSK modulation format. For the first two types, if the length of a selected path exceeds a distance limit, the required number of FSs become four and seven, respectively. The simulation results for the NSF network with demand type distribution (1) $(\rho_1, \rho_2, \rho_3) = (0.2, 0.5, 0.3)$ and (2) $(\rho_1, \rho_2, \rho_3) = (0.5, 0.3, 0.2)$ are shown in Figs. 24 and 25, respectively. We can see that our NSA algorithm still performs better than other baselines. The performance improvement is relatively small in Fig. 24 due to the domination of large-size requests.

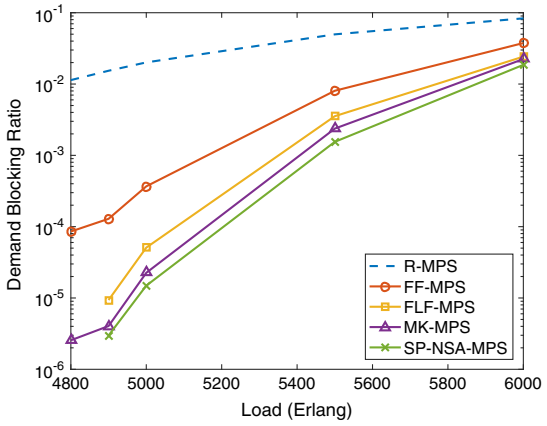


Fig. 24. Comparison of joint schemes in NSFNET with the uniform traffic pattern, demand type distribution (1), and two modulation levels.

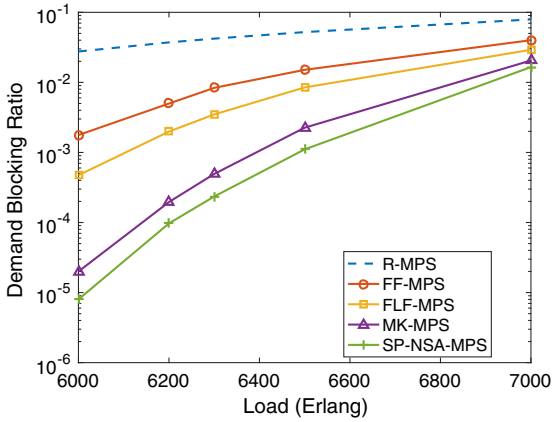


Fig. 25. Comparison of joint schemes in NSFNET with the uniform traffic pattern, demand type distribution (2), and two modulation levels.

## VI. Conclusion

We present a new approach for solving the routing and spectrum assignment problem for dynamic heterogeneous traffic requests in elastic optical networks with multiple fibers per link. The new approach has three novel components to it: multipath selection to fully utilize the path diversity of the network, spectrum partitioning with resource sharing to mitigate spectrum fragmentation without sacrificing resource utilization, and next-state-aware slot assignment that minimizes the reduction of network capacity after assignment. Through extensive simulation results, we show that our algorithm, which combines these three features, exhibits much better performance than several baseline algorithms and other algorithms in the literature.

## Acknowledgment

This work was supported by NSF grants 1406971, 1813617, and 1818858. The authors gratefully acknowledge valuable discussions with Maotong Xu.

## References

[1] M. Jinno, H. Takara, B. Kozicki, Y. Tsukishima, Y. Sone, and S. Matsuoka, "Spectrum-efficient and scalable elastic optical path network: Architecture, benefits, and enabling technologies," *IEEE Commun. Mag.*, vol. 47, no. 11, pp. 66–73, 2009.

[2] Y. Wang, X. Cao, and Y. Pan, "A study of the routing and spectrum allocation in spectrum-sliced elastic optical path networks," in *Proc. IEEE INFOCOM*, 2011, pp. 1503–1511.

[3] B. C. Chatterjee, N. Sarma, and E. Oki, "Routing and spectrum allocation in elastic optical networks: A tutorial," *IEEE Commun. Surv. Tutorials*, vol. 17, no. 3, pp. 1776–1800, 2015.

[4] J. Wu, S. Subramaniam, and H. Hasegawa, "Comparison of OXC node architectures for WDM and flex-grid optical networks," in *24th Int. Conf. on Computer Communication and Networks (ICCCN)*, 2015, pp. 1–8.

[5] K. Christodoulopoulos, I. Tomkos, and E. A. Varvarigos, "Routing and spectrum allocation in OFDM-based optical networks with elastic bandwidth allocation," in *Global Telecommunications Conf. (GLOBECOM)*, 2010, pp. 1–6.

[6] J. Wu, M. Xu, S. Subramaniam, and H. Hasegawa, "Routing, fiber, band, and spectrum assignment (RFBSA) for multi-granular elastic optical networks," in *IEEE Int. Conf. on Communications (ICC)*, 2017, pp. 1–6.

[7] J. Wu, M. Xu, S. Subramaniam, and H. Hasegawa, "Joint banding-node placement and resource allocation for multi-granular elastic optical networks," in *IEEE Global Communications Conf. (GLOBECOM)*, 2017, pp. 1–6.

[8] S. Shirazipourazad, C. Zhou, Z. Derakhshandeh, and A. Sen, "On routing and spectrum allocation in spectrum-sliced optical networks," in *Proc. IEEE INFOCOM*, 2013, pp. 385–389.

[9] M. Jinno, B. Kozicki, H. Takara, A. Watanabe, Y. Sone, T. Tanaka, and A. Hirano, "Distance-adaptive spectrum resource allocation in spectrum-sliced elastic optical path network [Topics in Optical Communications]," *IEEE Commun. Mag.*, vol. 48, no. 8, pp. 138–145, 2010.

[10] K. Christodoulopoulos, I. Tomkos, and E. Varvarigos, "Elastic bandwidth allocation in flexible OFDM-based optical networks," *J. Lightwave Technol.*, vol. 29, no. 9, pp. 1354–1366, 2011.

[11] M. Zhang, C. You, H. Jiang, and Z. Zhu, "Dynamic and adaptive bandwidth defragmentation in spectrum-sliced elastic optical networks with time-varying traffic," *J. Lightwave Technol.*, vol. 32, no. 5, pp. 1014–1023, 2014.

[12] Y. Sone, A. Hirano, A. Kadohata, M. Jinno, and O. Ishida, "Routing and spectrum assignment algorithm maximizes spectrum utilization in optical networks," in *37th European Conf. and Exhibition on Optical Communication (ECOC)*, 2011, pp. 1–3.

[13] Z. Zhu, W. Lu, L. Zhang, and N. Ansari, "Dynamic service provisioning in elastic optical networks with hybrid single-/multi-path routing," *J. Lightwave Technol.*, vol. 31, no. 1, pp. 15–22, 2013.

[14] X. Chen, J. Li, P. Zhu, R. Tang, Z. Chen, and Y. He, "Fragmentation-aware routing and spectrum allocation scheme based on distribution of traffic bandwidth in elastic optical networks," *J. Opt. Commun. Netw.*, vol. 7, no. 11, pp. 1064–1074, 2015.

[15] C.-F. Hsu, Y.-C. Chang, and S.-C. Sie, "Graph-model-based dynamic routing and spectrum assignment in elastic optical networks," *J. Opt. Commun. Netw.*, vol. 8, no. 7, pp. 507–520, July 2016.

[16] A. N. Patel, P. N. Ji, J. P. Jue, and T. Wang, "Routing, wavelength assignment, and spectrum allocation algorithms in transparent flexible optical WDM networks," *Opt. Switching Netw.*, vol. 9, no. 3, pp. 191–204, 2012.

[17] M. Zhang, W. Shi, L. Gong, W. Lu, and Z. Zhu, "Bandwidth defragmentation in dynamic elastic optical networks with minimum traffic disruptions," in *IEEE Int. Conf. on Communications (ICC)*, 2013, pp. 3894–3898.

[18] R. Wang and B. Mukherjee, "Spectrum management in heterogeneous bandwidth networks," in *Global Communications Conf. (GLOBECOM)*, 2012, pp. 2907–2911.

[19] R. Wang and B. Mukherjee, "Spectrum management in heterogeneous bandwidth optical networks," *Opt. Switching Netw.*, vol. 11, pp. 83–91, 2014.

[20] W. Fadini and E. Oki, "A subcarrier-slot partition scheme for wavelength assignment in elastic optical networks," in *IEEE 15th Int. Conf. on High Performance Switching and Routing (HPSR)*, 2014, pp. 7–12.

[21] Cisco Visual Networking Index: Forecast and Trends, 2017–2022, White Paper, 2018 [Online]. Available: http://www.cisco.com.

[22] S. Subramaniam and R. A. Barry, "Wavelength assignment in fixed routing WDM networks," in *IEEE Int. Conf. on Communications (ICC)*, 1997, vol. 1, pp. 406–410.

[23] X. Zhang and C. Qiao, "Wavelength assignment for dynamic traffic in multi-fiber WDM networks," in *7th Int. Conf. on Computer Communications and Networks*, 1998, pp. 479–485.

[24] S. Xu, L. Li, S. Wang, and C. Chen, "Wavelength assignment for dynamic traffic in WDM networks," in *IEEE Int. Conf. on Networks (ICON)*, 2000, pp. 375–379.

[25] S. Xu, L. Li, and S. Wang, "Dynamic routing and assignment of wavelength algorithms in multifiber wavelength division multiplexing networks," *IEEE J. Sel. Areas Commun.*, vol. 18, no. 10, pp. 2130–2137, 2000.

[26] G. Li and R. Simha, "On the wavelength assignment problem in multifiber WDM star and ring networks," in *19th Annu. Joint Conf. of the IEEE Computer and Communications Societies (INFOCOM)*, 2000, vol. 3, pp. 1771–1780.

[27] K. Liu, "Routing and wavelength assignment algorithm in multi-fiber WDM optical networks," in *Symp. on Photonics and Optoelectronics (SOPO)*, 2009, pp. 1–4.

[28] A. Coiro, M. Listanti, A. Valenti, and F. Matera, "Power-aware routing and wavelength assignment in multi-fiber optical networks," *J. Opt. Commun. Netw.*, vol. 3, no. 11, pp. 816–829, 2011.

[29] Y. Hirota, H. Tode, and K. Murakami, "Multi-fiber based dynamic spectrum resource allocation for multi-domain elastic optical networks," in *OptoElectronics and Communications Conf.*, 2013.

[30] J. Wu, S. Subramaniam, and H. Hasegawa, "Dynamic routing and spectrum assignment for multi-fiber elastic optical networks," in *Photonic Networks and Devices*, 2018, paper NeTu4F-1.

[31] Z.-S. Shen, T. Kusano, H. Hasegawa, and K.-I. Sato, "A novel routing and frequency slot assignment scheme that can adapt to transmission speed migration," in *Optical Fiber Communication Conf.*, 2015, paper W1I-2.

[32] D. Amar, E. Le Rouzic, N. Brochier, E. Bonetto, and C. Lepers, "Traffic forecast impact on spectrum fragmentation in gridless optical networks," in *European Conf. on Optical Communication (ECOC)*, 2014, pp. 1–3.

[33] F. Morales, M. Ruiz, and L. Velasco, "Incremental capacity planning in optical transport networks based on periodic performance metrics," in *18th Int. Conf. on Transparent Optical Networks (ICTON)*, 2016, pp. 1–4.